nature Vol 457 | 8 January 2009 | doi:10.1038/nature07610

LETTERS

Measured long-range repulsive Casimir–Lifshitz forces

J. N. Munday[1], Federico Capasso[2] & V. Adrian Parsegian[3]

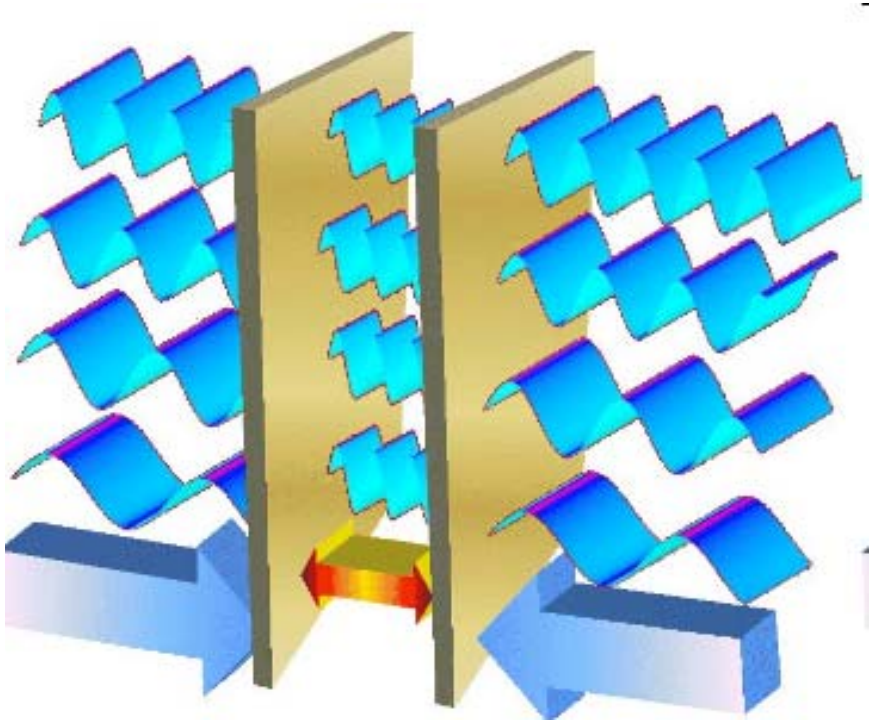

Fundamental curiousity for Nature.

Practical application for microscopic levitation.

Virtual Particles...

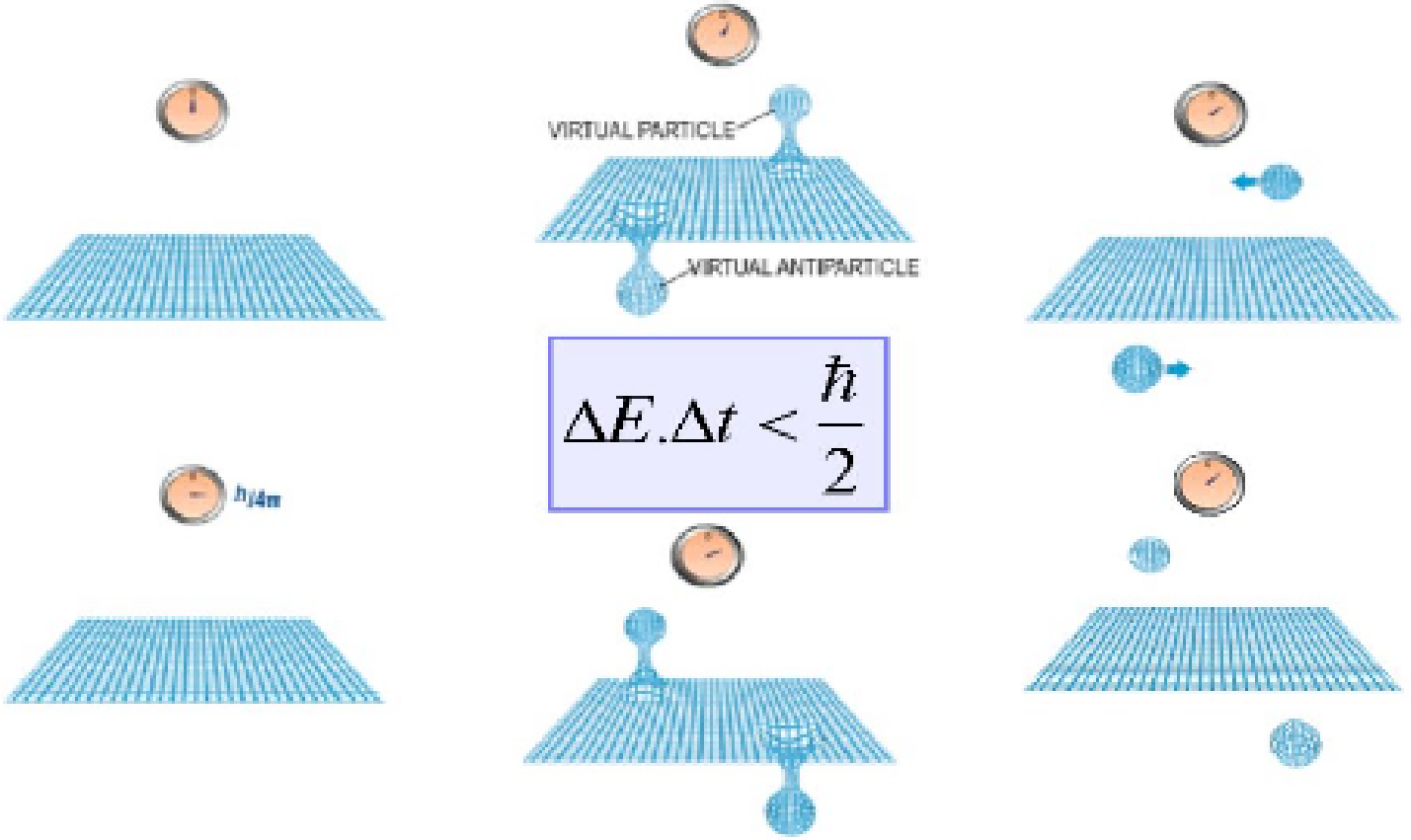

Vacuum space is very active due to a quantum effect!

Precision Measurement of the Casimir Force from 0.1 to 0.9 μm

(PRL Vol.81　1998)

M.Hasegawa
KUHEP colloquium
Dec. 21 2004

Contents

1. Casimir force について
2. Casimir force 研究の背景
3. 本実験について
4. 考察

カシミール力（量子真空場ゼロ点振動力）

H.D.Casimirによって提唱

Proc.K.Ned.Akad Wet. 51, 793 (1948)

真空中の電磁場のゼロ点振動エネルギー　＝

　境界条件によって差を持つ
(たとえば右図の場合、金属板表面では電場は0になるので、許される状態が限られる）
→ 金属板内部に引力が生じる

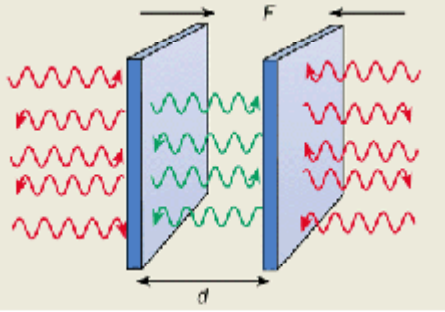

(次ページ)

カシミール力 (平行平板間)

金属板無し　　金属板有り

状態数　$2\frac{L^3}{(2\pi)^3}\int d\vec{k}$　　$2\frac{L^2}{(2\pi)^2}\sum_{n_z}\int dk_x dk_y$

$k_x=\frac{2\pi n_x}{L}, k_y=\frac{2\pi n_y}{L}, k_z=\frac{2\pi n_z}{L}$　　$k_x=\frac{2\pi n_x}{L}, k_y=\frac{2\pi n_y}{L}, k_z=\frac{\pi n_z}{d}$

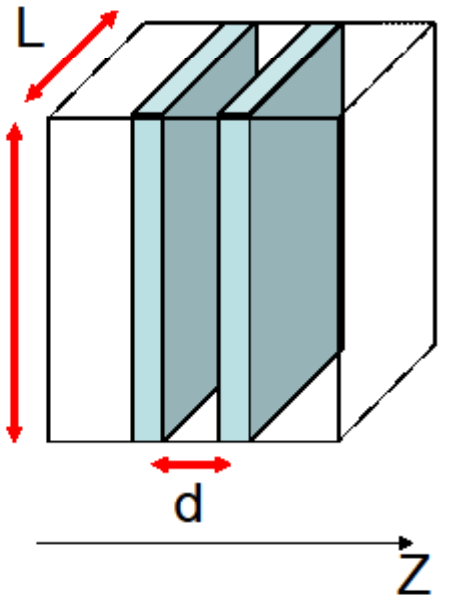

単位体積あたりのエネルギー

$$\frac{c\hbar}{(2\pi)^3}\int k d\vec{k} \qquad \frac{c\hbar}{(2\pi)^2}\frac{1}{d}\int dk_x dk_y \sum_{n_z} k$$

$$\Delta W = W(\text{有り}) - W(\text{無し})$$

$$= \frac{c\hbar\pi^2}{4d^4}\int_0^\infty d\rho\,\rho\left\{\sum_{n_z=0}^{\infty}\sqrt{\rho^2+n_z^2} - \int_0^\infty dz\sqrt{\rho^2+z^2}\right\}$$

$$= -\frac{c\hbar\pi^2}{48d^4}\int_0^\infty dx\frac{x^3}{e^x-1} = -\frac{c\hbar\pi^2}{720d^4}$$

$$F = -\frac{\partial}{\partial d}(\Delta V) = -\frac{\partial}{\partial d}(d\bullet\Delta W) = -\frac{c\hbar\pi^2}{240d^4}$$

それぞれ積分は発散するが
差をとると有限

計算に興味がある人は
ノート差し上げます。

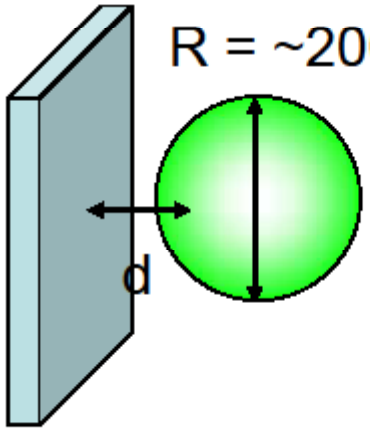

$$F = \frac{\pi^3 \hbar c}{360} \bullet \frac{R}{d^3} \sim \frac{0.6}{(d/1.0\mu m)^3} \times 10^{-12}\,[N]$$

AFMの測定限界 ~10^{-2} N/m

F > ~Å x k (cantileverの弾性定数)

~ 10^{-12} [N]

→ <1.0 μm での測定

AFM: Atomic Force Microscope

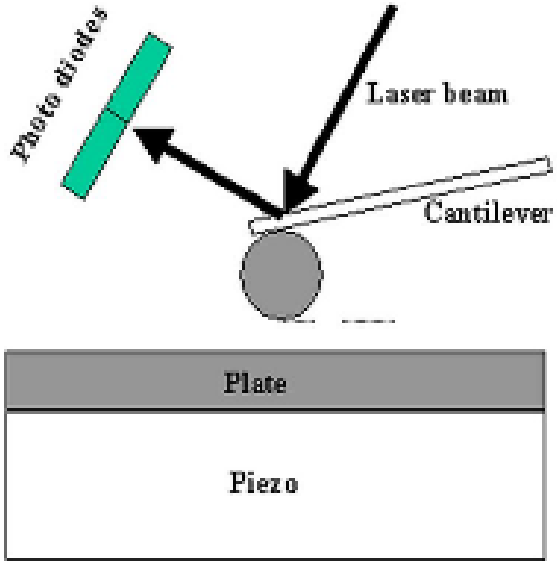

In Mohideen and Roy's experiment the force between an aluminium coated polystyrene sphere and an opticaly polished flat saphire disk (also aluminium coated) is measured by the deflection of a laser beam. The laser beam is reflected from the cantilever on which the sphere is mounted, and the position of the reflected beam determined by the output of a pair of photodiodes. A piezo stack is used to bring the flat disk close to the sphere.

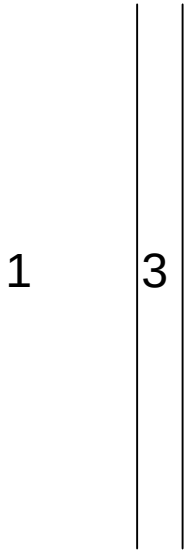

$$-(\varepsilon_1-\varepsilon_3)(\varepsilon_2-\varepsilon_3)$$

$$\varepsilon_1>\varepsilon_3>\varepsilon_2$$

The requirement for repulsive force.

Theory and calculations

Tabulated values for the optical properties of the materials are used for calculations. Data for gold and silica are from Ref[4]. Below $\omega = 0.125$ eV, data is not available for gold, so the Drude model is used:

$$\varepsilon(\omega) = 1 - \frac{\omega_p^{\,2}}{\omega(\omega + i\gamma)},$$

where ω_p=7.50 eV and γ=0.061 eV.[5] The dielectric functions are then evaluated at imaginary frequencies[6] $i\xi = i\frac{2\pi k_B T}{\hbar} m$, where m is a positive integer or zero, according to:

$$\varepsilon_i(i\xi) = 1 + \frac{\pi}{2}\int_{x=0}^{\infty} \frac{x\,\mathrm{Im}[\varepsilon_i(x)]}{x^2 + \xi^2} dx.$$

$\varepsilon(i\xi)$ corresponds to the continuation of $\varepsilon(\omega)$ in the complex plane and physically represents the material's response to exponentially increasing fields rather than oscillatory ones[7]. For bromobenzene, less data is available, and a two-oscillator model is used[8,9]:

$$\varepsilon(i\xi) = 1 + \frac{C_{IR}}{1 + \left(\xi / \omega_{IR}\right)^2} + \frac{C_{UV}}{1 + \left(\xi / \omega_{UV}\right)^2},$$

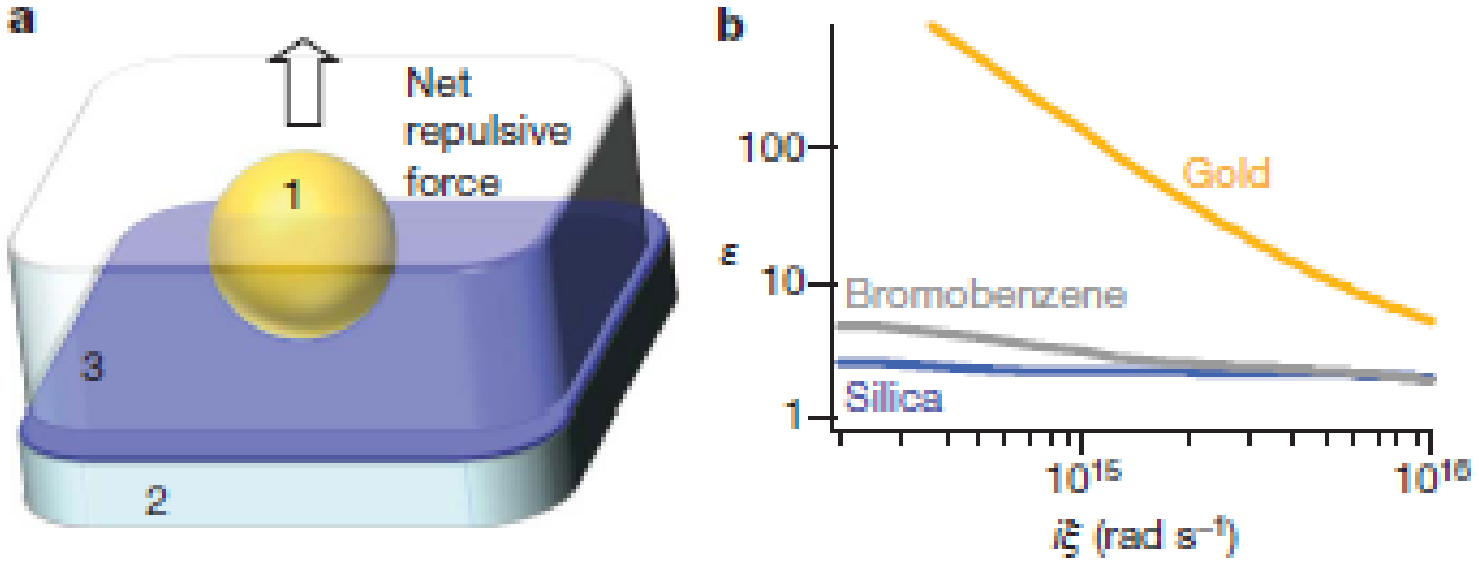

Figure 1 | Repulsive quantum electrodynamical forces can exist for two materials separated by a fluid. **a**, The interaction between material 1 and material 2 immersed in a fluid (material 3) is repulsive when $\varepsilon_1(i\xi) > \varepsilon_3(i\xi) > \varepsilon_2(i\xi)$, where the $\varepsilon(i\xi)$ terms are the dielectric functions at imaginary frequency (see Supplementary Information for details about the definition of $\varepsilon(i\xi)$). **b**, The optical properties of gold, bromobenzene and silica are such that $\varepsilon_{\text{gold}}(i\xi) > \varepsilon_{\text{bromobenzene}}(i\xi) > \varepsilon_{\text{silica}}(i\xi)$ and lead to a repulsive force between the gold and silica surfaces.

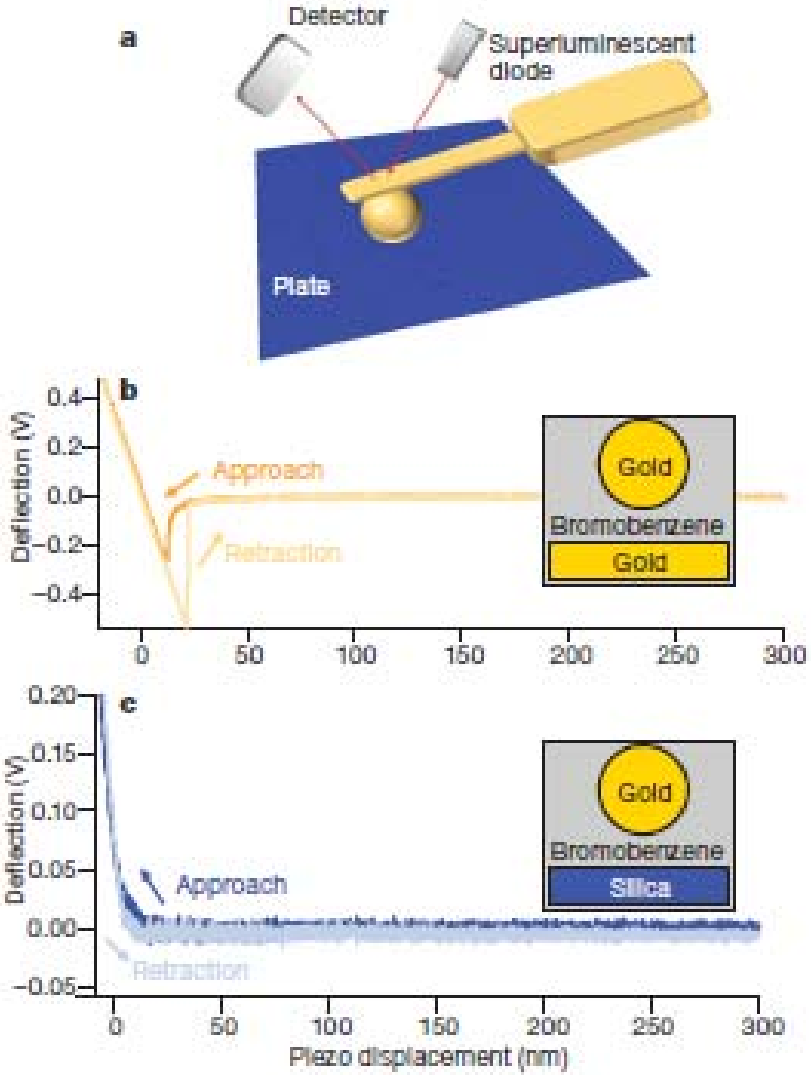

Figure 2 | Experimental set-up and deflection data. **a**, A sphere is attached to an atomic force microscope cantilever, which is enclosed within a bromobenzene-filled cell for force measurements. **b**, Deflection data showing attractive interactions between a gold sphere and a gold plate. **c**, For the case of the same gold sphere and a silica plate, deflection data show a repulsive interaction evident during both approach and retraction. Note that the deflection voltage signal is a difference signal obtained from the detector and is proportional to the bending of the cantilever, as discussed in the text.

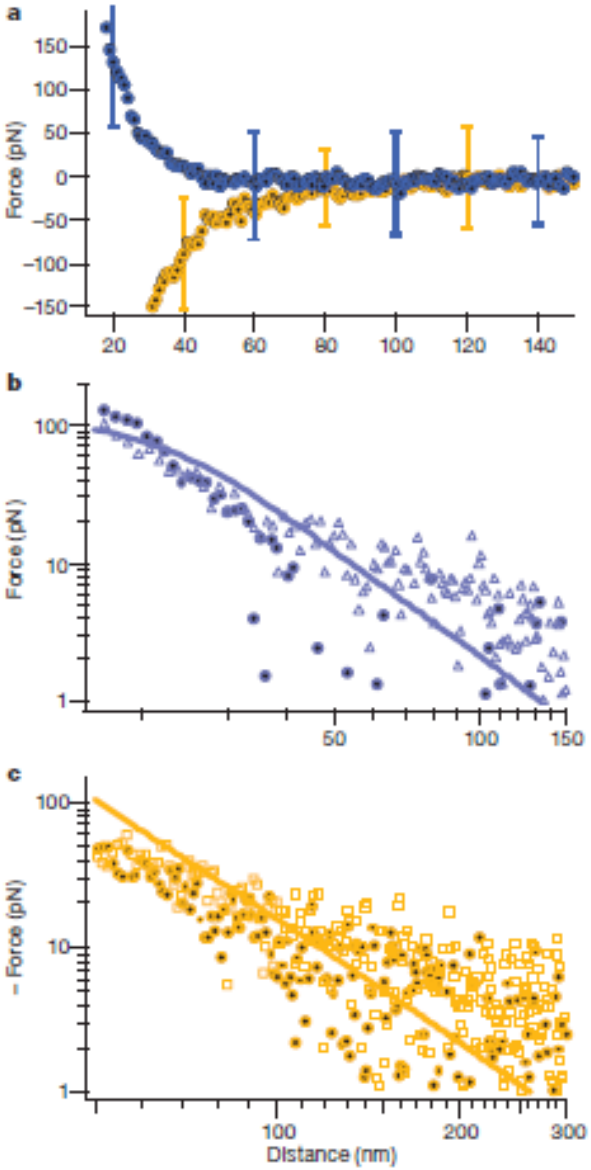

Figure 3 | Attractive and repulsive Casimir–Lifshitz force measurements. **a**, Blue (orange) circles represent the average of 50 data sets for the force between a gold sphere and a silica (gold) plate in bromobenzene. For clarity, error bars, which represent the standard deviation of the data, are only shown for seven data points. **b**, Measured repulsive force between a gold sphere and a silica plate in bromobenzene on a log–log scale (blue circles) and calculated force using Lifshitz's theory (solid line) including corrections for the measured surface roughness of the sphere and the plate. Blue triangles are force data for another gold sphere (nominally of the same diameter)/silica plate pair. **c**, Measured attractive force on a log–log scale for two gold sphere/plate pairs (circles and squares) in bromobenzene. The calculated force includes surface roughness corrections corresponding to the data represented by the circles (see Supplementary Information for calculations).

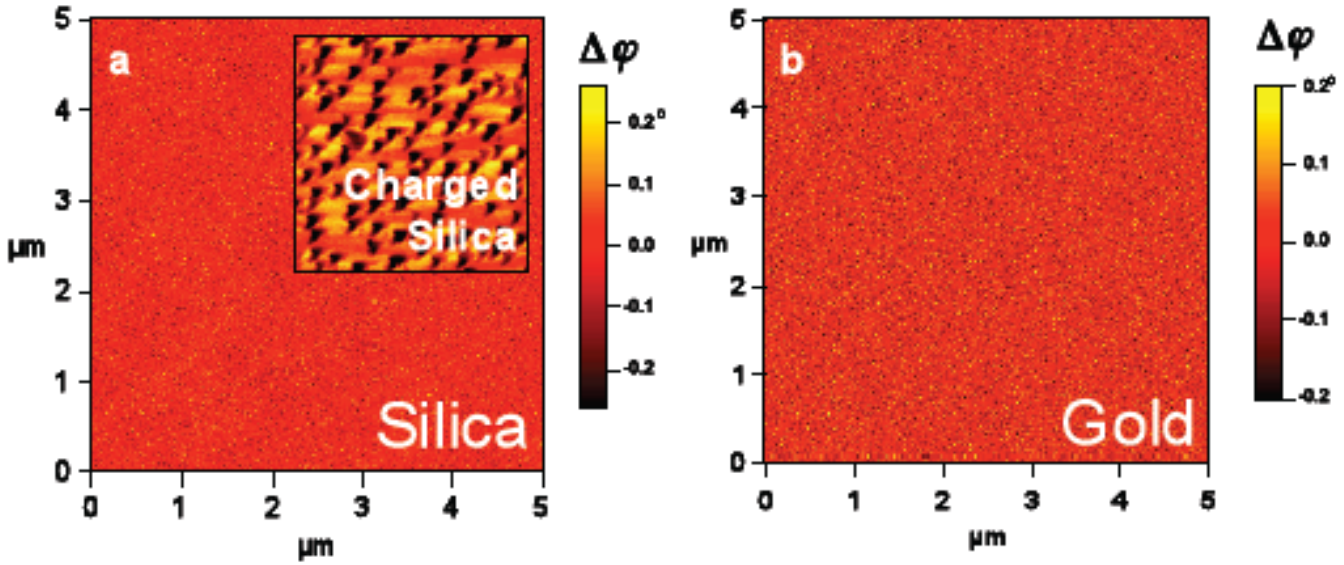

Fig. S1. With a standard conductive cantilever, electrostatic force microscopy is performed to ensure that the surfaces of both the silica (**a**) and gold (**b**) contain little charge variation after the cleaning procedure as determined by the spatial variation in the cantilever phase signal $\Delta\varphi$ with an applied voltage of 2 V at a distance 40 nm above the surface. An uncleaned silica sample exposed to electron irradiation from a scanning electron microscope shows clear contrast in the phase signal corresponding to patches of charge (inset **a**) for the same applied voltage.

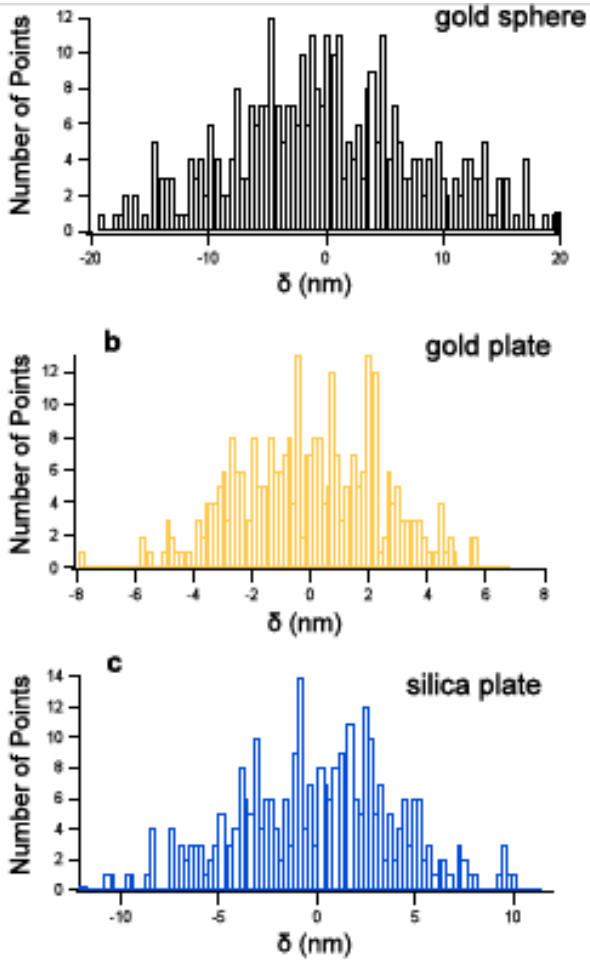

Fig. S2. Surface roughness measurements on the gold coated sphere (**a**), the gold coated plate (**b**), and the silica plate (**c**), as determined using an optical profiler. The bar heights represent the number of pixels with a displacement δ from an ideally smooth surface.

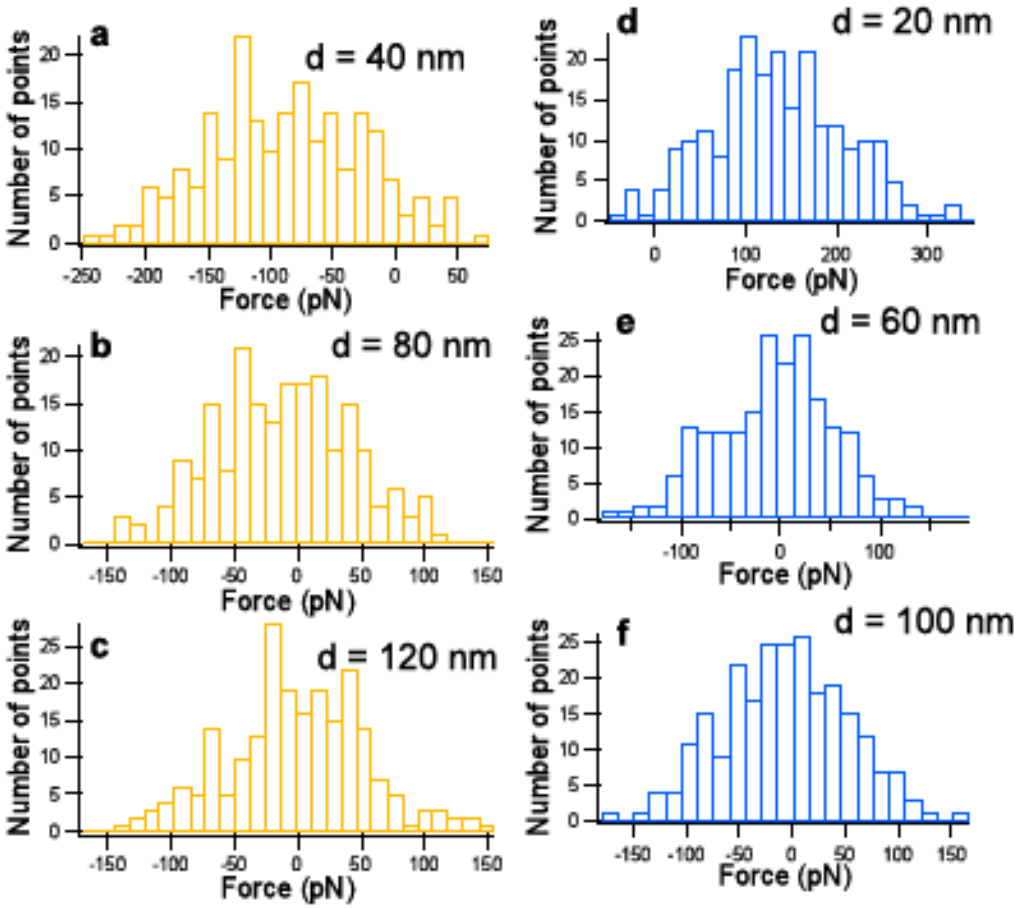

Fig. S3. Histograms of the force data show an approximately Gaussian distribution. Force data is collected from 50 runs, and distances are rounded to the nearest nm. Distributions are shown for the case of the gold sphere and gold plate (**a**,**b**,**c**) at three different sphere-plate separations. Similar data is shown for the case of the gold sphere and the silica plate (**d**,**e**,**f**).